

Research paper

PVDF–PZT nanohybrid based nanogenerator for energy harvesting applications

Shivaji H. Wankhade, Shivam Tiwari, Anupama Gaur, Pralay Maiti *

School of Materials Science and Technology, Indian Institute of Technology (Banaras Hindu University), Varanasi, 221005, India



ARTICLE INFO

Article history:

Received 17 October 2019

Received in revised form 14 January 2020

Accepted 5 February 2020

Available online xxxx

Keywords:

PVDF

PZT

Nanohybrid

Piezoelectricity

Energy harvesting

ABSTRACT

With the depletion of the conventional energy sources, measures are being taken to create an alternate energy sources for the future. Energy harvesting from different sources are one of the better steps taken in this direction. Mechanical energy harvesting from the waste mechanical source is gaining profound investigation. Here, a nanohybrid of poly(vinylidene fluoride) and lead zirconia titanate (PZT) is prepared through solution route for energy harvesting applications. PZT is synthesized using solid state route and its concentration was varied in the nanohybrid to get the best properties from the hybrid. Structural and morphological aspects of the nanohybrid have been explored for their suitable application. Device has been fabricated using the nanohybrid to convert the waste mechanical energy from various human motions to the useful electrical energy. The device is able to generate a maximum output voltage of 55 V and a power density of $36 \mu\text{Wcm}^{-2}$. The device is able to produce voltage output from different human motions such as finger tapping, feet tapping and bending. The mechanism of charge conversion is also discussed which explains the generation of such a high electrical output from waste mechanical source.

© 2020 Published by Elsevier Ltd. This is an open access article under the CC BY-NC-ND license (<http://creativecommons.org/licenses/by-nc-nd/4.0/>).

1. Introduction

With the increasing demand of energy and the depletion of the primary source of energy, the need to find the alternate source of energy has been the concern of the society. Mechanical energy harvesting is one of the alternate ways to generate energy from the waste mechanical sources. It is a process of converting vibrational, mechanical energy produced from different sources, which are otherwise wasted, into useful electrical energy. Gaur et al. (2018) Piezoelectric materials are best suited to exploit this vibrational energy into electrical signals. Piezoelectricity is a phenomenon in which spontaneous polarization occurs when a material is subjected to stress. Venkatragavaraj et al. (2001) Several categories of materials such as ceramics, polymers, alloys etc. possess piezoelectric properties which possess the potential for energy harvesting applications. Energy harvesting has mostly been done with high piezoelectric coefficient materials such as barium titanate (BaTiO_3) (Park et al., 2010), PZT (Anton and Sodano, 2007), and zinc oxide (ZnO) (Kumar and Kim, 2012). Despite of having high piezoelectric coefficient, they are very brittle in nature and difficult to process which makes them unsuitable for flexible application devices. To overcome these drawbacks of these ceramics, alternatives like polymeric materials are being used because of their flexibility. Wan and Bowen (2017)

Amongst the polymers, PVDF and its copolymers like PVDF–TrFE, PVDF–HFP shows better piezoelectric properties. Gaur et al. (2016, 2017) and Kumar et al. (2017) Despite of having low piezoelectric coefficients as compared to ceramic materials, slight modifications in the polymer or preparing a composite material with high piezoelectric coefficient materials may lead to better energy harvesting efficiency combined with flexibility and better mechanical strength (Alluri et al., 2017).

To attain the desired properties, fillers are added into the polymer matrix to achieve the combined properties of both matrix and fillers. For the preparation of composite material with high piezoelectric coefficients, fillers with high piezoelectric ceramics such as PZT, BaTiO_3 , ZnO (Shrout and Zhang, 2007) can be added to obtain relatively high coefficient value. Among all these materials, PZT shows better piezoelectric properties as compared to other ceramics/materials presented in supplementary Table S1. Piezoelectric constant of PZT is highest among all the available materials which can be prepared easily in its pure state at a lower cost. PZT has a perovskite structure ($\text{Pb}(\text{Zr}_{1-x}\text{Ti}_x)\text{O}_3$). It lies on the morphotropic phase boundary at $x = 0.48$ separating tetragonal and rhombohedral phase. (Shrout and Zhang, 2007)

Among the polymers PVDF is most suitable piezo polymers due to its features like chemical resistant (Gaur et al., 2017), radiation resistant (Tiwari et al., 2013), flexible (Alluri et al., 2017), biocompatible (Lee et al., 2014), low dielectric constant (Baur et al., 2014), and considerable piezoelectric, ferroelectric and pyroelectric properties which are best suited for energy harvesting

* Corresponding author.

E-mail address: pmaiti.mst@itbhu.ac.in (P. Maiti).

applications. PVDF is a semi crystalline polymer and crystallizes mainly into five different phases α , β , γ , δ and ϵ . The α -phase is a non-electroactive phase having TGT \bar{G} conformation which leads to its non-polar nature. While β -phase has all trans (TTTT) conformation and thus behaves as polar phase, while the γ - phase is somewhat polar in nature due to its T₃GT₃ \bar{G} conformation. Gaur et al. (2017) On performing some modification in pure PVDF the non-electroactive phase can be transformed into electroactive polar β -phase (Tiwari et al., 2019). The piezo-active β phase possesses TTTT (all trans) conformation which accounts for most of its piezoelectric properties. Due to this ability of transformation of non-electroactive phases to piezoelectric active phase draws supplementary attention towards PVDF for energy harvesting applications. Scheinbeim et al. (1979) Some of the works has been reported earlier based on PVDF for energy harvesting applications such as Siddiqui et al. used BaTiO₃ as filler in P(VDF-TrFE) and produced an output of 3.4 V and 27.4 μ W/cm³ power using finger tapping (Siddiqui et al., 2016). Filler like MWCNT in PVDF have generated maximum voltage of 6 V and a power of 81.8 nW (Yu et al., 2013). Output voltage of 1.6 V and 0.03 μ W power from electrospun PVDF-PZT nanohybrid was reported in the literature (Chen et al., 2010). It is important to mention that although carbon nanotubes (CNTs) are well known for their high aspect ratio, good electrical conductivity and good mechanical properties, and such advantages can enable their composites to have electromechanical sensing transduction mechanisms once CNTs are embedded as fillers there are challenges that they must be dealt with in the dispersion and characterization on a volumetric scale that is completely different from the nanoscale. The incorporation of CNTs into PVDF not only improves the electrical conductivity that facilitates the charge mobility but also affects the β phase of PVDF, consequently enhancing the piezoelectric properties of nanogenerator.

In the present work, (Pb(Zr_(1-x)Ti_x)O₃) with $x = 0.48$ is chosen based on the previous work as at this morphotropic phase boundary, it exhibits excellent piezoelectric and dielectric properties. Shrout and Zhang (2007) PZT is synthesized using a solid-state route and pure phase obtained is used as filler in nanohybrid. Nanohybrid of PVDF and PZT is prepared through solution casting method which was molded to film form for energy harvesting application. Device has been fabricated using nanohybrid after proper electroding and encapsulation and electromechanical responses of the device is measured for its usage in day to day life activities for energy generation from waste mechanical resources.

2. Experimental

2.1. Materials

Commercial grade SOLEF 6008 poly(vinylidene fluoride) having $M_w = 2.7 \times 10^5$, PDI = 2.1, density = 1.98 g/cc was used for the experimental study and was supplied by Ausimont, Italy. Commercial PbO and ZrO₂ (HIMEDIA) were used. Commercial TiO₂ from EVONIK Industries was used as it received. Dimethyl formamide of spectroscopic grade was used as common solvent and was purchased from Merck, India.

2.2. Filler preparation

Appropriate amount of PbO, ZrO₂, TiO₂ were weighed and taken to form desired Pb(Zr_{0.52}Ti_{0.48})O₃. These oxides were mixed and hand milled for about one hour. This milled powder was calcined at 800 °C for 6 h. The calcined powder was crushed nicely and then pellet was prepared and sintered at 1150 °C for 4 h. After sintering, the pellets were characterized using XRD to confirm the phase purity of PZT.

2.3. Nanohybrid preparation

Initially PVDF was mixed with DMF in a beaker and was stirred at 60 °C until it gets dissolved completely. Meanwhile, PZT was mixed with DMF in different beaker and was stirred at 60 °C followed by ultrasonication. The sonicated PZT dispersion and viscous PVDF solution were mixed and kept for stirring at 60 °C till the solution becomes homogenous. Then solution is transferred to petri dish and kept overnight at 60 °C for drying. This dried film is compressed in compression molding machine to get a homogenous film of the hybrid material. By using this method, the nanohybrids are prepared using different concentrations of filler in 0, 10, 20, 30, 40 wt% and are assigned them as P, P-P10, P-P20, P-P30, P-P40, respectively.

2.4. Device fabrication

From the prepared homogenous film, a rectangular film is cut and on both sides conducting layer of silver is applied using brush for making the surface conducting and the electrodes are attached. The dimension of the prepared device is 2 × 0.9 cm². The prepared device is enclosed in PDMS poly (dimethyl siloxane) (PDMS: Sylgard, 184 silicone elastomer) and curing agent (10:1 wt/wt) and kept in vacuum oven at 55 °C for 2 h. The PDMS layer was used to provide the flexibility and stability to the device avoiding any interaction with the hybrid specimen.

3. Characterization

X-ray diffraction (XRD): Structural analysis of PZT and nanohybrid was done by using X-ray Diffractometer at room Temperature. X-ray Diffractometer used in measurement was Rigaku Mini-flex 600 operating at current 15 mA and voltage of 40 kV.

Differential scanning calorimetry (DSC): To measure the melting temperature and heat of fusion of PVDF and nanohybrid DSC measurements were performed using DSC (Mettler 832). The characterization was performed from 30–200 °C at 10°/min.

Polarized optical microscopy (POM): To examine the morphology of film, it was subjected to optical microscope POM (Leitz Biomed). Reflectance mode was used in the characterization of pure polymer and its nanohybrid under room temperature.

Scanning electron microscopy (SEM): To examine the surface morphology of PVDF and nanohybrid precisely, SEM was done. The samples were coated with gold before observation under SEM to make the surface conducting. Scanning electron microscope used was SUPRA 40, Zeiss.

Atomic force microscopy (AFM): The atomic force microscopy (NTEGRA Prima, NT-MDT) was used to observe exactly the morphology of nanohybrid. All the measurements in AFM were done in semi contact mode.

Thermogravimetric analyses (TGA): The thermogravimetric analyzer (Mettler Toledo) was used to examine the degradation temperature of pure PVDF and nanohybrid. The TGA was performed at a temperature range of 30–600 °C with the scan rate of 10°/min.

Electromechanical Response: The fabricated devices was subjected to different types of stresses generated by human body such as finger tapping, feet tapping, and bending to measure the voltage generated by these devices using Tektronix TBS 1072B digital storage oscilloscope. Variable resistance box was used to calculate the power generated by the devices. The Dielectric measurement was analyzed using Keysight E4990A having range from 20 Hz to 10 MHz. The measurement was performed in room temperature for all the samples. The mechanical properties were measured using Instron universal testing machine at a strain rate of 5 mm/min at room temperature.

4. Results and discussion

4.1. Structure and morphology

Fig. 1a shows the XRD patterns of PVDF and PZT ceramic particles having concentration $Zr/Ti = 52/48$. The XRD pattern reveals a phase pure perovskite of PZT (Zak et al., 2011). The XRD pattern of pure PVDF shows peaks at 17.7° , 18.4° , 20.0° , 26.7° , and 38.5° which are predominant α -phase peaks of PVDF (Kumar et al., 2019; Gaur et al., 2018). Whereas, the nanohybrid shows the peaks corresponding to α -phase of PVDF as well as the diffraction peaks of PZT which are at 22.1° , 26.7° , and 31.3° . A comparative pattern of XRD of nanohybrids at different PZT loading is shown in supporting information (Figure S1).

Pure PVDF consists of mainly α -phase which possesses spherulitic morphology as seen from the polarized optical micrograph (POM). Incorporation of fillers to the PVDF matrix leads to some morphological alterations which is clearly seen in case of POM images of P-P30 (nanohybrid containing 30% PZT) (Fig. 1b). The addition of PZT powder to the PVDF matrix results in the reduction of spherulite dimension indicating the nucleating effect of PZT. The morphological analysis at higher magnification is performed using SEM which also confirms the observations obtained from POM (large spherulite in pure PVDF against tiny one in nanohybrid) (Fig. 1c). Similarly, the agglomerated PZT nanoparticles can be seen in AFM image of nanohybrid, which is absent in pure PVDF. Aftab et al. (2013) Relatively, rough surface is observed in nanohybrid against smoother surface in pure PVDF. Two different surfaces are observed which is confirmative of the morphological changes.

The DSC shows the melting behavior of PVDF and P-P30 nanohybrid in the Fig. 2a. Pure PVDF shows the melting temperature at 170.1 and 174°C which are melting point of α -phase. Gaur et al. (2017) Double melting endotherm is presumably due to melt recrystallization. On the other hand, melting temperature of P-P30 nanohybrid is 168.4 and 173.6°C and slight reduction in temperature is due to interaction between PZT and PVDF. The DSC thermograms of the nanohybrids at different PZT concentrations are shown in supporting information (Figure S3). The enthalpy (heat of fusion) of pure PVDF and P-P30 are 27.1 and 18.6 J g^{-1} , respectively (Dong et al., 2010). The reduction in enthalpy suggests that considerable interaction exist between PZT and PVDF.

To determine the thermal stability and degradation of the prepared films, TGA analyses are done at heating rate of $20^\circ/\text{min}$. Fig. 2b shows the TGA thermograms of pure PVDF and P-P30 nanohybrid. PVDF film is very stable up to 420°C followed by sudden weight loss indicative of thermal degradation. The nanohybrid film P-P30 also shows thermal stability up to 420°C and there is no change of degradation temperature in presence of PZT (Revathi et al., 2017). Hence, there is no change of thermal stability and structure of PVDF in presence of PZT. The mechanical properties of the P and P-P 30 were measured at room temperature (supplementary Figure S4). The toughness values of P and P-P 30 are 35.2 ± 0.5 and $106.5 \pm 0.8\text{ MJ/m}^3$, respectively. It is clear that incorporation of PZT leads to increase in the mechanical property as suggested from the above observations.

4.2. Electromechanical responses

It is clear from the structural studies that after adding electroactive filler to the polymer, the nanohybrid becomes electroactive material which is suitable for energy harvesting application and proper device made out of nanohybrid can convert waste mechanical energy to useful electrical energy. A device has been

fabricated using hybrid films to measure the electromechanical response under human body motion. Devices prepared using these materials are encapsulated in poly (dimethyl siloxane) (PDMS) to protect the device and give dimensional stability. Encapsulation provides better rigidity and it also protects the device and its electrode from direct impact. Fig. 3a shows the schematic diagram of the device where the composite is coated with silver for electroding purpose and copper wires were used to connect it to external circuit. The output voltage of the material is measured with different human movements such as finger tapping, feet tapping and bending. Fig. 3b shows the output voltages of 5, 20, 40 and 55 V (peak-to peak) from P, P-P10, P-P20, and P-P30, respectively, on finger tapping. The maximum stress applied to the device while imparting the finger pressure was $\sim 8.5\text{ KPa}$ as calculated in the supporting information based on previous reports. Gaur et al. (2019) This indicates that the output voltage increases by increasing the electroactive filler concentration. But, after 30 wt% concentration of the filler, the output voltage of the nanohybrid decreases which may be due to the agglomeration of the nanoparticle or due to improper dispersion of filler in PVDF matrix. Hence, from the obtained output, we can optimize that the P-P30 provides maximum output voltage using finger tapping as compared to other filler containing nanohybrids. The application of periodic mechanical force produces mechanical strain in the hybrid which in turn induces polarization in the device (Chang et al., 2010). Due to this induced polarization, potential develops across the material which causes the charge carriers (electrons) to flow through external circuit where load is present to balance the electric field produce in the materials. Thus, an electrical signal is generated from a piezoelectric material. When the mechanical force is released, it cause potential drop immediately due to which electron gather to electrode and flows back to it producing a reverse signal (Karan et al., 2016).

The power density is measured using load in external circuit which can be calculated using the formula $P = V^2/(R_L \times A)$, where, P is the power density, V is the maximum output voltage, R_L is load resistance across the device and A is area of the hybrid film. The power density of the device increases with increase in concentration of electroactive filler (after 30 wt% loading of filler power reduces) as shown in Fig. 3c and maximum power density is exhibited by P-P30 of $36\ \mu\text{W cm}^{-2}$ with a maximum peak to peak voltage of 55 V as compared to pure PVDF which shows maximum power density of $1.35\ \mu\text{W cm}^{-2}$ with a maximum peak to peak voltage of 5.5 V. The obtained value is much higher as compared to reported values in literature. The Piezoelectric fiber composites (PFC) consisting of PZT fibers and PVDF matrix showed a power output of $11\ \mu\text{W}$ (Swallow et al., 2008). Whereas the output power of PZT nanofibers with PVDF polymer matrix showed power value of $0.03\ \mu\text{W}$ (Chen et al., 2010). The measured dielectric constant of P, P-P 30 and PZT powder was around 4.5, 10.2 and 1965, respectively (Figure S5). There was considerable rise in dielectric constant values for PZT based nanohybrids as compared to pure PVDF, which supports the above observations. Zak et al. (2011) The durability of the device (P-P30) was measured for longer span of time (Figure S6). From the durability plot it was confirmed that the device produced almost similar data over longer period of time without much fluctuations, which suggests the durability and stability of the device. Gaur et al. (2019)

There is distortion of lattice in hybrid when a mechanical stress is applied which creates a net dipole moment in the system. So, under pressure upon the hybrid such as finger tapping, walking, etc. results into change in dipole moment which generates charge that flows through external circuit providing electrical signal from the piezoelectric nanohybrid. This vibration creates voltage difference across electrodes due to charge separation

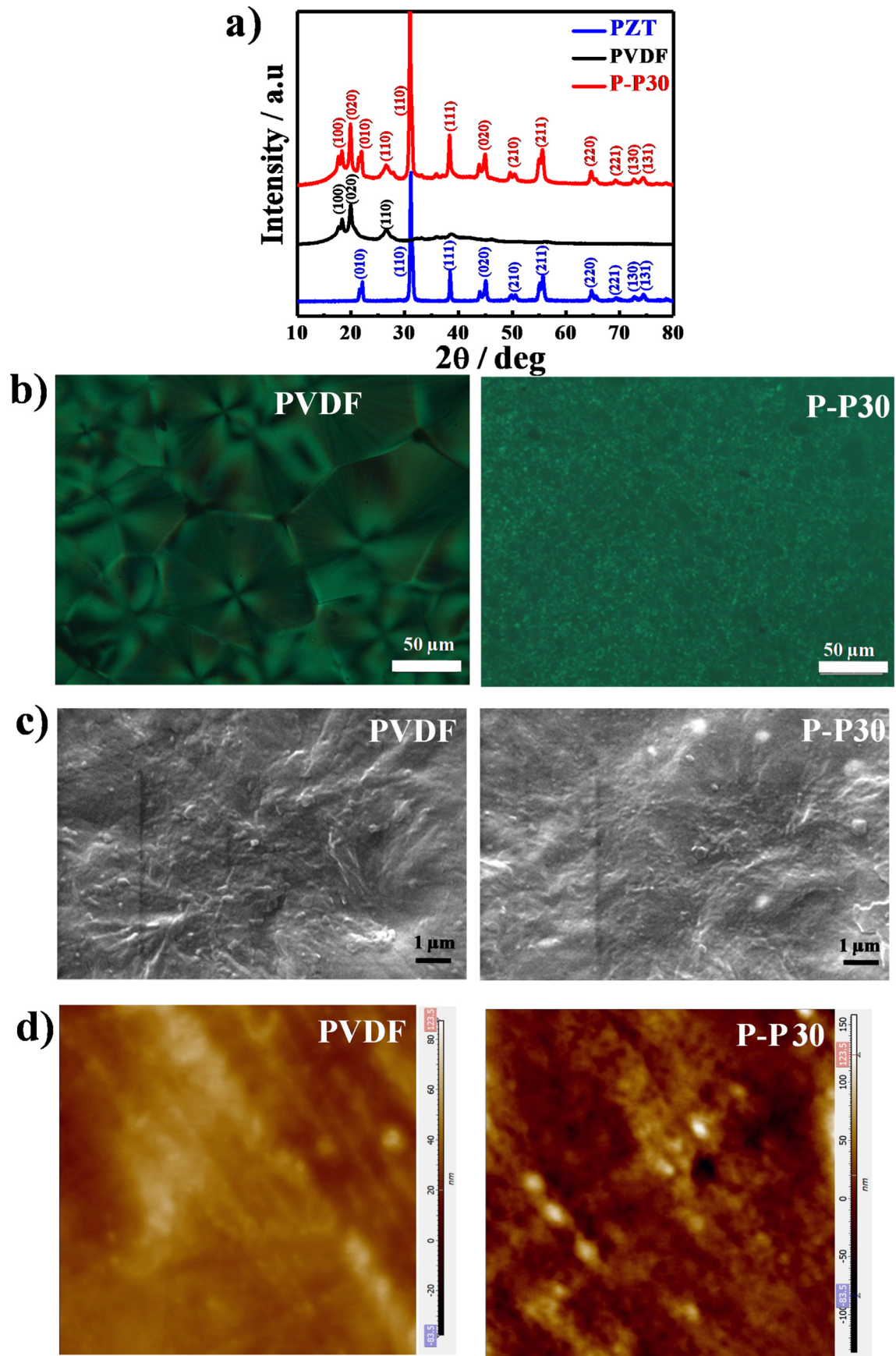


Fig. 1. (a) XRD patterns of pure PZT, PVDF and P-P30 nanohybrid; (b) Optical images of pristine PVDF and its nanohybrid P-P30; (c) SEM micrographs of PVDF and P-P30; and (d) AFM images of the prepared films of PVDF and P-P30 nanohybrid.

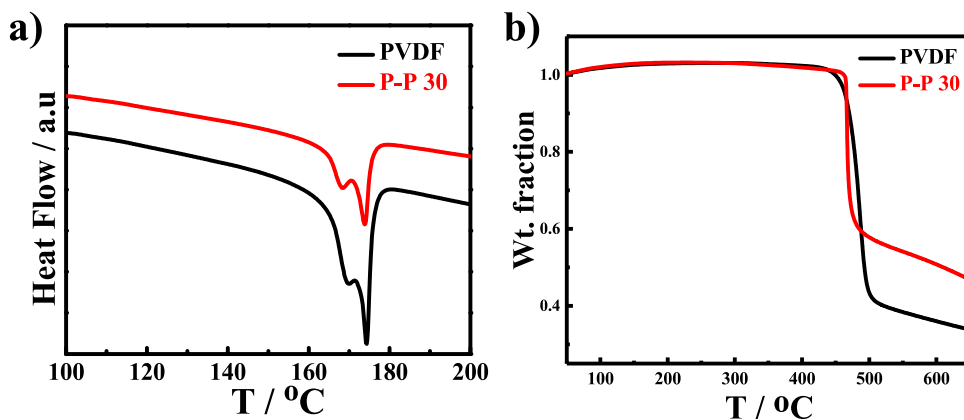


Fig. 2. (a) DSC thermographs showing the different melting temperature of the different phases of PVDF and P-P 30 and (b) TGA plot showing the degradation behavior of the PVDF and P-P 30.

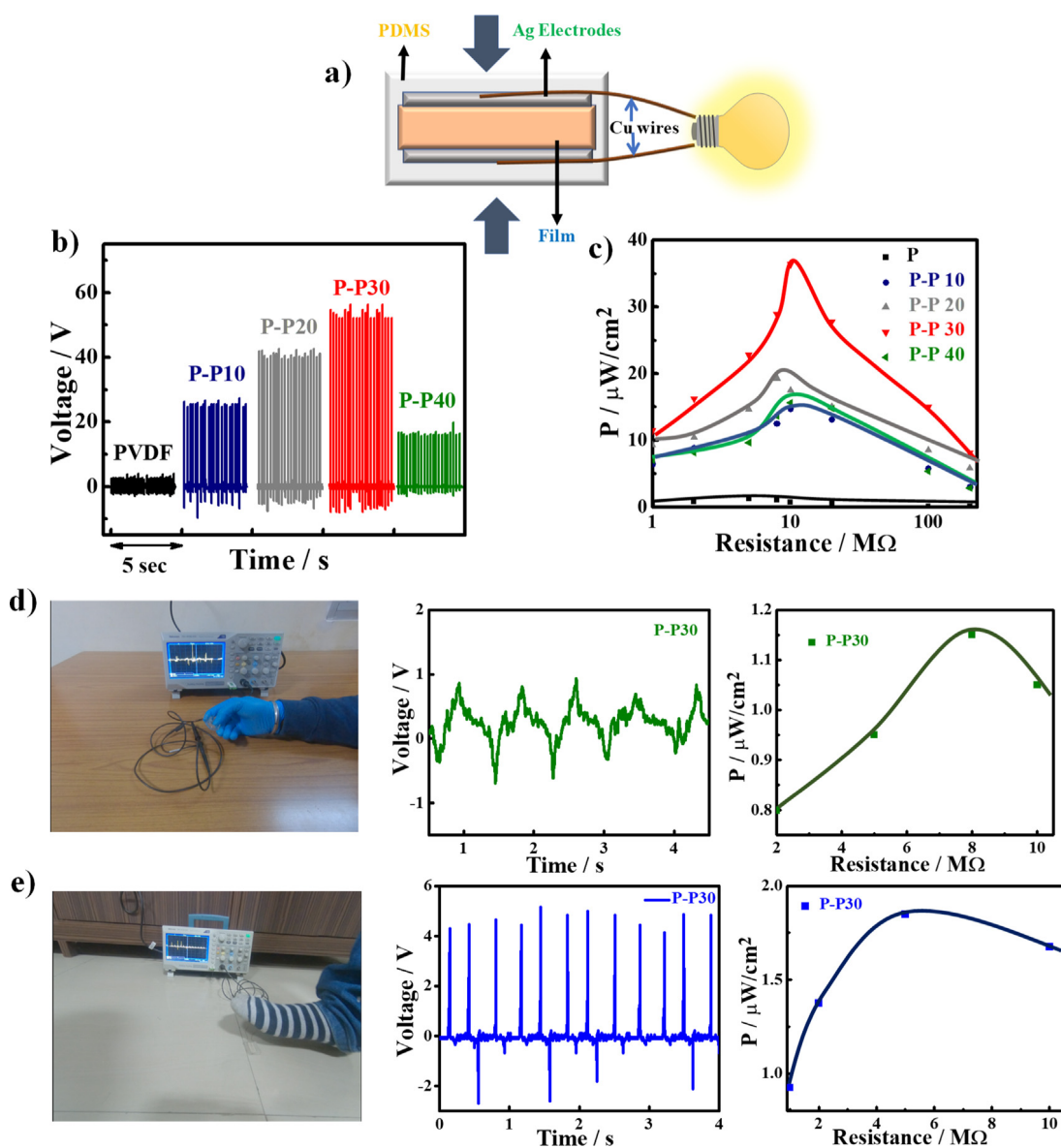


Fig. 3. (a) Schematic representation of the device; (b) Output voltage comparison of different nanohybrids with pure PVDF on application of finger tapping; (c) comparative power density of the pristine PVDF and its nanohybrids at different PZT loading; Output voltage and power density measured through; (d) bending; and (e) feet tapping and associated voltage generation and power density from respective mode of force application.

at constant strain net charge balances with piezoelectric bound charges due to which potentials difference across electrodes become zero. Tiwari et al. (2019) and Chen et al. (2010) Fig. 3d, e shows the output voltage and power density measured across external resistance produced via bending and foot tapping method. Maximum output voltage generated from the bending and feet tapping modes are around 1.5 and 5.5 V, respectively. The generated power density values for bending and foot tapping mode are measured to be 1.15 and 1.8 $\mu\text{W}/\text{cm}^{-2}$, respectively. A video VS1 of voltage generation from different modes has been provided in supporting information.

Now, it is clear that by increasing electroactive filler content there is increase in output voltage and power significantly (restricted up to 30 wt%). The presence of electroactive filler leads to the separation of charge by its inherent piezoelectric property. The output produced by hybrid materials is much higher than pristine PVDF film and recently reported data in energy harvesting field. This device can convert energy from different human motion into electrical energy. This hybrid film is encapsulated in poly(dimethyl siloxane) (PDMS), which play vital role in transferring of stress to the hybrid as well as giving sufficient rigidity and protection to the electrode. The fabrication and assembly of device is very simple and economic also the device is very stable due to encapsulation in PDMS. Thus, this device is very useful for energy conversion and can be used to operate the low power consuming electronic devices.

5. Conclusion

Easily fabricated, durable, cheap and efficient energy harvesting device is fabricated using PVDF and PZT nanohybrid systems. The device shows very high electrical output due to presence of electroactive filler and maximum output is generated using 30 wt.% of piezo-filler. This device produces output voltage of 55 V and output power density of 36 $\mu\text{W}/\text{cm}^{-2}$, which is considerably higher than the reported values for energy harvesting applications. Many other modes such as bending and feet tapping generates considerable amount of electrical output from the device made of nanohybrid. The mechanism behind the charge separation is discussed which helps to explain the reason behind exhibiting such high energy conversion. The miniature device can be used to operate some low power consumption electronic devices. Structural and thermal stability of the nanohybrid has been worked which is suitable for energy harvesting device applications.

Declaration of competing interest

The authors declare that they have no known competing financial interests or personal relationships that could have appeared to influence the work reported in this paper.

Acknowledgment

The author acknowledges the institute, IIT (BHU) VARANASI, India for financial assistant.

Appendix A. Supplementary data

Supplementary material related to this article can be found online at <https://doi.org/10.1016/j.egy.2020.02.003>.

References

- Aftab, S., Hall, D.A., Aleem, M.A., Siddiq, M., 2013. Low field ac study of PZT/PVDF nano composites. *J. Mater. Sci. Mater. Electron.* <http://dx.doi.org/10.1007/s10854-012-0861-z>.
- Alluri, N.R., Chandrasekhar, A., Jeong, J.H., Kim, S.J., 2017. Enhanced electroactive β -phase of the sonication-process-derived PVDF-activated carbon composite film for efficient energy conversion and a battery-free acceleration sensor. *J. Mater. Chem. C* <http://dx.doi.org/10.1039/c7tc00568g>.
- Anton, S.R., Sodano, H.A., 2007. A review of power harvesting using piezoelectric materials (2003–2006). *Smart Mater. Struct.* <http://dx.doi.org/10.1088/0964-1726/16/3/R01>.
- Baur, C., Apo, D.J., Maurya, D., Priya, S., Voit, W., 2014. Advances in piezoelectric polymer composites for vibrational energy harvesting. *ACS Symp. Ser.* <http://dx.doi.org/10.1021/bk-2014-1161.ch001>.
- Chang, C., Tran, V.H., Wang, J., Fuh, Y.K., Lin, L., 2010. Direct-write piezoelectric polymeric nanogenerator with high energy conversion efficiency. *Nano Lett.* <http://dx.doi.org/10.1021/nl9040719>.
- Chen, X., Xu, S., Yao, N., Shi, Y., 2010. 1.6 v nanogenerator for mechanical energy harvesting using PZT nanofibers. *Nano Lett.* <http://dx.doi.org/10.1021/nl100812k>.
- Dong, L., Li, R., Xiong, C., Quan, H., 2010. Effect of heat treatment on the electrical properties of lead zirconate titanate/poly (vinylidene fluoride) composites. *Polym. Int.* <http://dx.doi.org/10.1002/pi.2780>.
- Gaur, A., Kumar, C., Shukla, R., Maiti, P., 2017. Induced piezoelectricity in poly(vinylidene fluoride) hybrid as efficient energy harvester. *ChemistrySelect* 2, 8278–8287. <http://dx.doi.org/10.1002/slct.201701780>.
- Gaur, A., Kumar, C., Tiwari, S., Maiti, P., 2018. Efficient energy harvesting using processed poly(vinylidene fluoride) nanogenerator. *ACS Appl. Energy Mater.* <http://dx.doi.org/10.1021/acsaem.8b00483>.
- Gaur, A., Shukla, R., Kumar, B., Pal, A., Chatterji, S., Ranjan, R., Maiti, P., 2016. Processing and nanoclay induced piezoelectricity in poly(vinylidene fluoride-co-hexafluoro propylene) nanohybrid for device application. *Polymer (Guildf)* <http://dx.doi.org/10.1016/j.polymer.2016.05.049>.
- Gaur, A., Tiwari, S., Kumar, C., Maiti, P., 2019. A bio-based piezoelectric nanogenerator for mechanical energy harvesting using nanohybrid of poly(vinylidene fluoride). *Nanoscale Adv.* 1, 3200–3211. <http://dx.doi.org/10.1039/c9na00214f>.
- Karan, S.K., Bera, R., Paria, S., Das, A.K., Maiti, S., Maitra, A., Khatua, B.B., 2016. An approach to design highly durable piezoelectric nanogenerator based on self-poled PVDF/AlO-rGO flexible nanocomposite with high power density and energy conversion efficiency. *Adv. Energy Mater.* <http://dx.doi.org/10.1002/aenm.201601016>.
- Kumar, C., Gaur, A., Rai, S.K., Maiti, P., 2017. Piezo devices using poly(vinylidene fluoride)/reduced graphene oxide hybrid for energy harvesting. *Nano-Struct. Nano-Objects* <http://dx.doi.org/10.1016/j.nanoso.2017.10.006>.
- Kumar, C., Gaur, A., Tiwari, S., Biswas, A., Rai, S.K., Maiti, P., 2019. Bio-waste polymer hybrid as induced piezoelectric material with high energy harvesting efficiency. *Compos. Commun.* <http://dx.doi.org/10.1016/j.coco.2018.11.004>.
- Kumar, B., Kim, S.W., 2012. Energy harvesting based on semiconducting piezoelectric ZnO nanostructures. *Nano Energy* <http://dx.doi.org/10.1016/j.nanoen.2012.02.001>.
- Lee, B.S., Park, B., Yang, H.S., Han, J.W., Choong, C., Bae, J., Lee, K., Yu, W.R., Jeong, U., Chung, U.I., Park, J.J., Kim, O., 2014. Effects of substrate on piezoelectricity of electrospun poly(vinylidene fluoride)-nanofiber-based energy generators. *ACS Appl. Mater. Interfaces* <http://dx.doi.org/10.1021/am405684m>.
- Park, K., Il, Xu, S., Liu, Y., Hwang, G.T., Kang, S.J.L., Wang, Z.L., Lee, K.J., 2010. Piezoelectric BaTiO₃ thin film nanogenerator on plastic substrates. *Nano Lett.* <http://dx.doi.org/10.1021/nl102959k>.
- Revathi, S., Kennedy, L.J., Basha, S.K.K., Padmanabhan, R., 2017. Synthesis, structural, optical and dielectric properties of nanostructured 0–3 PZT/PVDF composite films. *J. Nanosci. Nanotechnol.* <http://dx.doi.org/10.1166/jnn.2018.15336>.
- Scheinbeim, J., Nakafuku, C., Newman, B.A., Pae, K.D., 1979. High-pressure crystallization of poly(vinylidene fluoride). *J. Appl. Phys.* 50, 4399–4405. <http://dx.doi.org/10.1063/1.326429>.
- Shrout, T.R., Zhang, S.J., 2007. Lead-free piezoelectric ceramics: Alternatives for PZT? *J. Electroceram.* <http://dx.doi.org/10.1007/s10832-007-9047-0>.
- Siddiqui, S., Kim, D., Il, Roh, E., Duy, L.T., Trung, T.Q., Nguyen, M.T., Lee, N.E., 2016. A durable and stable piezoelectric nanogenerator with nanocomposite nanofibers embedded in an elastomer under high loading for a self-powered sensor system. *Nano Energy* <http://dx.doi.org/10.1016/j.nanoen.2016.10.034>.
- Swallow, L.M., Luo, J.K., Siores, E., Patel, I., Dodds, D., 2008. A piezoelectric fibre composite based energy harvesting device for potential wearable applications. *Smart Mater. Struct.* <http://dx.doi.org/10.1088/0964-1726/17/2/025017>.
- Tiwari, S., Gaur, A., Kumar, C., Maiti, P., 2019. Enhanced piezoelectric response in nanoclay induced electrospun PVDF nanofibers for energy harvesting. *Energy* <http://dx.doi.org/10.1016/j.energy.2019.01.043>.

- Tiwari, V.K., Prasad, A.K., Singh, V., Jana, K.K., Misra, M., Prasad, C.D., Maiti, P., 2013. Nanoparticle and process induced super toughened piezoelectric hybrid materials: The effect of stretching on filled system. *Macromolecules* <http://dx.doi.org/10.1021/ma400603h>.
- Venkatragavaraj, E., Satish, B., Vinod, P.R., Vijaya, M.S., 2001. Piezoelectric properties of ferroelectric PZT-polymer composites. *J. Phys. D. Appl. Phys.* 34, 487–492. <http://dx.doi.org/10.1088/0022-3727/34/4/308>.
- Wan, C., Bowen, C.R., 2017. Multiscale-structuring of polyvinylidene fluoride for energy harvesting: the impact of molecular-, micro- and macro-structure. *J. Mater. Chem. A* <http://dx.doi.org/10.1039/c6ta09590a>.
- Yu, H., Huang, T., Lu, M., Mao, M., Zhang, Q., Wang, H., 2013. Enhanced power output of an electrospun PVDF/MWCNTs-based nanogenerator by tuning its conductivity. *Nanotechnology* <http://dx.doi.org/10.1088/0957-4484/24/40/405401>.
- Zak, A.K., Gan, W.C., Majid, W.H.A., Darroudi, M., Velayutham, T.S., 2011. Experimental and theoretical dielectric studies of PVDF/PZT nanocomposite thin films. *Ceram. Int.* 37, 1653–1660. <http://dx.doi.org/10.1016/j.ceramint.2011.01.037>.